PROTEIN STRUCTURE REPORT

Crystal structure of human proteasome assembly chaperone PAC4 involved in proteasome formation

Eiji Kurimoto,[1]* Tadashi Satoh,[2,3] Yuri Ito,[1] Eri Ishihara,[1] Kenta Okamoto,[2] Maho Yagi-Utsumi,[2,4] Keiji Tanaka,[5] and Koichi Kato[2,4]*

[1]Faculty of Pharmacy, Meijo University, Tempaku-ku, Nagoya, 468-8503, Japan

[2]Graduate School of Pharmaceutical Sciences, Nagoya City University, Mizuho-ku, Nagoya 467-8603, Japan

[3]JST, PRESTO, Mizuho-ku, Nagoya 467-8603, Japan

[4]Okazaki Institute for Integrative Bioscience and Institute for Molecular Science, National Institutes of Natural Sciences, Myodaiji, Okazaki, Aichi 444-8787, Japan

[5]Laboratory of Protein Metabolism, Tokyo Metropolitan Institute of Medical Science, Setagaya-ku, Tokyo 156-8506, Japan

Received 21 December 2016; Accepted 28 February 2017
DOI: 10.1002/pro.3153
Published online 6 March 2017 proteinscience.org

Abstract: The 26S proteasome is a large protein complex, responsible for degradation of ubiquinated proteins in eukaryotic cells. Eukaryotic proteasome formation is a highly ordered process that is assisted by several assembly chaperones. The assembly of its catalytic 20S core particle depends on at least five proteasome-specific chaperones, i.e., proteasome-assembling chaperons 1–4 (PAC1–4) and proteasome maturation protein (POMP). The orthologues of yeast assembly chaperones have been structurally characterized, whereas most mammalian assembly chaperones are not. In the present study, we determined a crystal structure of human PAC4 at 1.90-Å resolution. Our crystallographic data identify a hydrophobic surface that is surrounded by charged residues. The hydrophobic surface is complementary to that of its binding partner, PAC3. The surface also exhibits charge complementarity with the proteasomal α4–5 subunits. This will provide insights into human proteasome-assembling chaperones as potential anticancer drug targets.

Keywords: assembly chaperone; crystal structure; PAC4; proteasome

Additional Supporting Information may be found in the online version of this article.

Grant sponsor: Okazaki ORION project and Grants-in-Aid for Scientific Research; Grant numbers: JP15H02491 and JP25102008 to K.K.; Grant sponsor: Ministry of Education, Culture, Sports, Science and Technology, Japan.

Kenta Okamoto current address is The laboratory of Molecular Biophysics, Department of Cell and Molecular Biology, Uppsala University, Husargatan 3, Uppsala 75123, Sweden

*Correspondence to: Eiji Kurimoto, Ph.D., Faculty of Pharmacy, Meijo University, 150 Yagotoyama, Tempaku-ku, Nagoya 468-8503, Japan. E-mail: kurimoto@meijo-u.ac.jp or Koichi Kato, Ph.D., Okazaki Institute for Integrative Bioscience and Institute for Molecular Science, National Institutes of Natural Sciences, 5-1 Higashiyama, Myodaiji, Okazaki, Aichi 444-8787, Japan. E-mail: kkatonmr@ims.ac.jp

Introduction

The 26S proteasome plays a central role in selective ubiquitin-dependent protein degradation in eukaryotic cells.[1–3] This enzyme complex comprises a 20S core particle (CP) and one or two 19S regulatory particles (RPs). The catalytic 20S CP is built up with seven homologous α-subunits (α1–α7) and seven homologous β-subunits (β1–β7), forming a cylindrical architecture with arrangement of two distal α-subunit heteroheptameric rings and two proximal β-subunit heteroheptameric rings ($\alpha_{1-7}\beta_{1-7}\beta_{1-7}\alpha_{1-7}$). The β1, β2, and β5 subunits carries proteolytic active sites that are located on the inner surfaces of the β-ring, which acts as a chambered protease.[4,5] The 19S RP is constituted from a base subcomplex, comprising six ATPase subunits and a lid subcomplex, comprising at least 13 non-ATPase subunits.[6,7] This 19S RP is responsible for capturing ubiquitin-tagged substrates, for opening the gated pore of the 20S CP, and for deubiquitinating and unfolding the substrates.[1–3,8,9]

The assembly of the eukaryotic 26S proteasome is not spontaneous but is mediated by several assembly chaperones.[8–10] A correct arrangement of the proteasomal subunits is required for functioning of the eukaryotic proteasome. This is attained through transient and proper interactions among the chaperones and the proteasomal subunits during the proteasome biogenesis. The formation of the eukaryotic 20S CP is assisted by five proteasome-specific assembly chaperones, namely PAC1–PAC4 in human (Pba1–Pba4 in yeast) and POMP (Ump1). As for 19S RP assembly, four assembly chaperones—p27 (Nas2), gankyrin (Nas6), PAAF1 (Rpn14), and S5b (Hsm3)—are responsible for an efficient and precise formation of the base subcomplex.

During the last decade, extensive structural studies on the CP- and RP-assembly chaperones[11–17] have elucidated their specific interactions with cognate proteasomal subunits. For example, yeast Pba3 and Pba4 are structurally similar and form a heterodimer, which thereby acts as a matchmaker, facilitating the interaction between α4 and α5, a crucial step in α-ring formation.[17–19] Since the proteasome expression level is highly upregulated in cancer cells,[20] it is demanded to develop inhibitors that merely target the proteasome biogenesis without affecting mature proteasomes in other normal cells. Proteasome-assembling chaperones are potential targets of inhibiting accurate proteasome assembly[21,22]; therefore, the structural information on human proteasome-assembling chaperones is crucial for designing and developing less toxic anticancer drugs. However, to date, most of the structural data on the proteasome-assembling chaperones have been limited to yeast proteins, with modest sequence identities with the human counterparts (<20%, as in the case of Pba1–Pba4). Regarding the mammalian proteasome-assembling chaperones, the structural data have been available only for human PAC3[17] and mouse gankyrin.[11] Hence, we performed X-ray crystallographic analysis for determining the structure of the human PAC4.

Results and Discussion

PAC4 structure

We purified recombinant PAC4 protein and crystalized it using the hanging-drop vapor diffusion method. To avoid unfavorable protein aggregation via intermolecular disulfide bonds in the recombinant protein preparation, a C55S mutation was introduced into PAC4. While bacterially expressed PAC3 was homodimeric,[17] the recombinant PAC4 protein existed both as monomeric and homodimeric forms [Supporting Information Fig. S1(A)], the latter of which was successfully crystallized. Crystal structure of the PAC4 dimer was solved by the single-anomalous dispersion (SAD) and molecular replacement methods using crystals of non-labeled and selenomethionine (SeMet)-labeled proteins. The final model of PAC4, refined to a 1.90-Å resolution, had R_{work} and R_{free} values of 20.5% and 25.3%, respectively (Table I). The crystal belongs to the space group *F*222 with four molecules per asymmetric unit. The structures of the four molecules are very similar to one another with a root-mean-square deviation (rmsd) value of 0.34–0.50 Å for superimposed 98–99 Cα atoms. The PAC4 formed a domain-swapped homodimer related by a pseudo two-folded symmetry [Fig. 1(A)].

Structural Comparison with Other Proteasome Assembly Chaperones

To confirm structural similarities among PAC4 and its homologs, we compared the structure of PAC4 with those of its yeast ortholog Pba4, its binding partner PAC3, and Pba3, the yeast ortholog of PAC3. Although sequence similarities among these proteins are very low (13.8–18.3% identities), the overall tertiary structure of PAC4 is essentially identical to those of PAC3, Pba3, and Pba4 [Fig. 1(B)], suggesting their common fold. The rmsd values of superimposed 89–96 Cα atoms between PAC4 and the homologs are 1.89–2.19 Å. Each PAC4 protomer exhibits a globular structure that comprises a six-stranded β-sheet (termed S1–S6) and two α-helices (termed H1 and H2) [Fig. 1(A)]. Two antiparallel β-sheets are made up with three β-strands (S1–S3 and S4–S6) [Fig. 1(B)]. The parallel β-strand interaction between two antiparallel β-sheets of PAC4 and Pba4 is mediated by S3 and S6 sheets [Fig. 1(B)]. In the PAC4 structure, this β-strand interaction is supposed to be weak because domain-swapping occurs between the antiparallel β-sheet units. Among these proteins, the yeast ortholog Pba4 adopts the most similar structure to PAC4. However, there are

Table I. *Data Collection and Refinement Statistics for PAC4*

	Native	SeMet
Crystallographic data		
Space group	*F*222	$P4_32_12$
Unit cell parameters		
a, b, c (Å)	72.6, 152.8, 212.9	129.0, 129.0, 72.8
Data processing statistics		
Beamline	SPring-8 BL44XU	SPring-8 BL44XU
Wavelength (Å)	0.90000	0.97932
Resolution range (Å)	50–1.90 (1.93–1.90)	50–2.60 (2.64–2.60)
Number of total reflections	343,113	273,692
Number of unique reflections	46,618	19,649
Completeness (%)	99.8 (100.0)	99.9 (100.0)
R_{merge} (%)	8.7 (80.0)	13.1 (94.2)
$I / \sigma(I)$	42.0 (3.3)	50.6 (7.6)
Redundancy	7.4 (7.5)	13.9 (14.6)
Refinement statistics		
Resolution range (Å)		
R_{work}/R_{free} (%)	20.5/25.3	
R.m.s.d. bond length (Å) and angles (°)	0.018/1.86	
Ramachandran plot (%)		
Most favored regions	92.1	
Additional allowed regions	6.9	
Generously allowed	1.0	
Number of molecules		
Protein atoms (A/B/C/D)	912/857/842/857	
Water molecules	287	
Ions	8	
Average *B*-values (Å^2)		
Protein atoms (A/B/C/D)	43.7/40.8/51.5/46.3	
Water molecules	47.8	
Ions	51.4	

prominent structural differences between PAC4 and Pba4 such as shortened S2–S3 loops, extended S1–S2 sheets, shortened S4–S6 sheets, and shortened H1 and H2 helices in the PAC4 [Fig. 1(B,C)].

Pba4 forms a heterodimer with Pba3 *in vitro* and *in vivo*.[17] We confirm that PAC4 is capable of making a heterodimer with PAC3 *in vitro* as shown by size exclusion chromatography [Supporting Information Fig. S1(B)], consistent with the previously reported interaction *in vivo*.[23] The Pba3–Pba4 heterodimer has a β-sandwich structure formed by two six-stranded β-sheets on their convex surfaces, which is similar to the domain-swapped homodimeric structure of PAC4 [Fig. 1(A)]. Pba4 interacts with Pba3 through hydrophobic interactions and surface-charge complementarity,[17] which includes one negatively and two positively charged patches in Pba4 and one positively and two negatively charged patches in Pba3 (Supporting Information Fig. S2). Our structure-based sequence alignment analysis indicated that the residues at the heterodimeric interface between yeast Pba3 and Pba4 are not well conserved in human PAC3 and PAC4 [Fig. 1(C)]. However, although the positions are different between the orthologs, the surface-charge complementarity is also found at the putative dimeric interface between PAC3 and PAC4 (Supporting Information Fig. S2). Hydrophobic patches are commonly found in the centers of β-sheet surfaces that forms the Pba3–Pba4 interface and, more extensively, the PAC3–PAC4 interface. These structural data suggest that PAC4 forms a heterodimeric complex with PAC3 through its hydrophobic surface surrounded by the charged residues. To characterize their interaction in solution, we conducted NMR analysis using PAC4 and ^{15}N-labled PAC3, in which the NMR data was previously obtained in our group.[21] As expected, upon addition of PAC4, significant spectral changes were observed for the residues involved in the homodimer formation in the PAC3 (Supporting Information Fig. S3). Based on the fact that PAC3–PAC4 and PAC3–PAC3 interactions were mediated by common interfaces, we constructed a PAC3-PAC4 docking model using program MOE and the PAC3 homodimer crystal structure (Supporting Information Fig. S4). In the docking model, the PAC3–PAC4 interface is created mainly through hydrophobic and charged residues. The dimeric interface of PAC3 can be a target of inhibitors against chaperone dimerization.[21] The present data offer structural foundation for designing inhibitors that target the dimeric interface of PAC4.

In the previous study, we presented a structural model in which the Pba3–Pba4 heterodimer acts as a matchmaker, reinforcing the interaction between the proteasomal α4 and α5 subunits.[17,18] In that

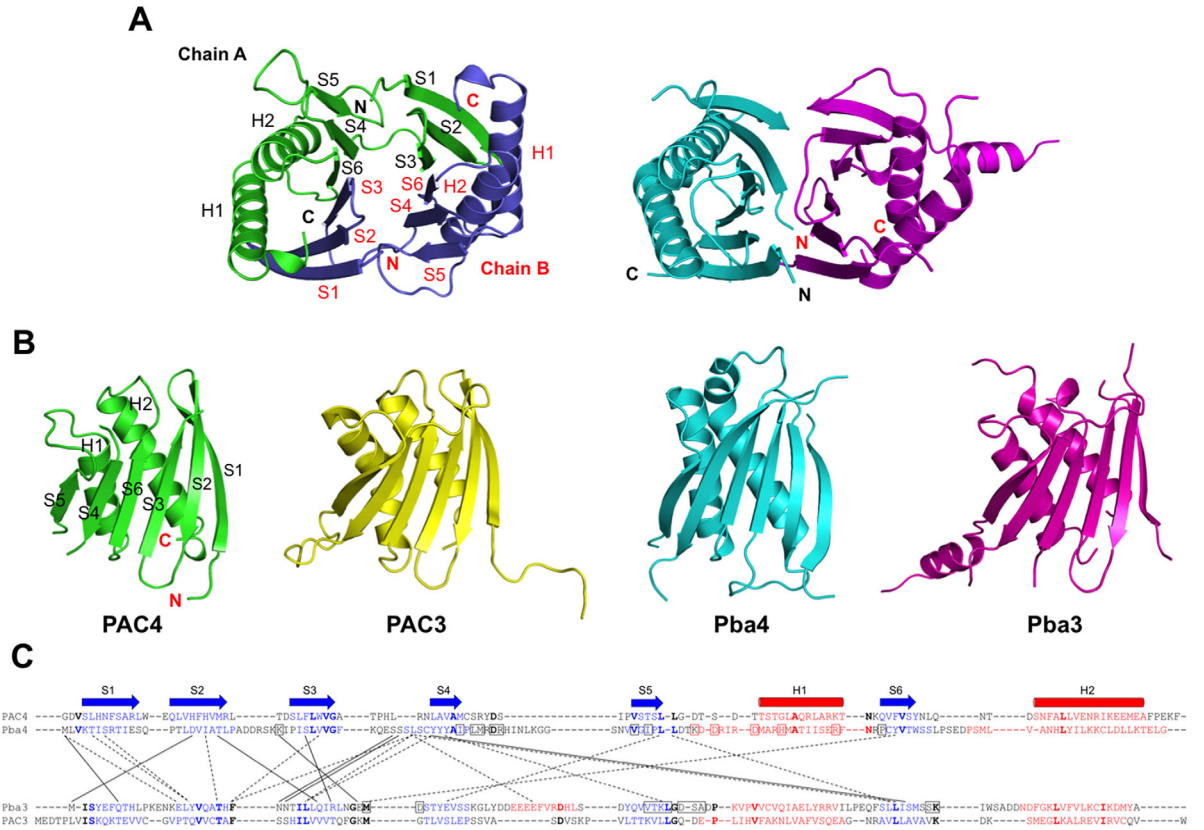

Figure 1. Comparison of overall structures of PAC4 homologs. (A) Crystal structures of domain-swapped PAC4 homodimer and Pba3–4 heterodimer. In the PAC4 structure (left), chains A and B are colored in green and slate, respectively. Positions of the N and C termini and secondary structure elements of domain-swapped PAC4 are indicated with black and red letters for chains A and B, respectively. Numbering of the β-strands is according to the scheme of *Saccharomyces cerevisiae* Pba4 (Dmp1/Poc4), Pba3 (Dmp2/Poc3), and human PAC3.[17] In the Pba3–Pba4 heterodimer structure (right, PDB code: 2Z5B), ribbon models of Pba4 and Pba3 are colored in cyan and magenta, respectively. http://imolecules3d.wiley.com/imolecules3d/review/8Gb8VSRcJezNWMySA6O7AbkJTkfUoWFlPlxl88NqyGYsKwbtMriwm0mrOdZy4Qom802/1583; http://imolecules3d.wiley.com/imolecules3d/review/8Gb8VSRcJezNWMySA6O7AbkJTkfUoWFlPlxl88NqyGYsKwbtMriwm0mrOdZy4Qom802/1584 (B) Monomeric structures of PAC4 homologs: human PAC4 (green) and PAC3 (yellow, 2Z5E, chain A); *S. cerevisiae* Pba4 (cyan, 2Z5B, chain A) and Pba3 (magenta, 2Z5B, chain B). For clarity, the globular structure of PAC4 containing residues 1–43 and 48–123 from chains A and B, respectively, are indicated. http://imolecules3d.wiley.com/imolecules3d/review/8Gb8VSRcJezNWMySA6O7AbkJTkfUoWFlPlxl88NqyGYsKwbtMriwm0mrOdZy4Qom802/1585 (C) Structure-based sequence alignment of PAC4, Pba4, PAC3, and Pba3. Secondary structure elements of PAC4 are indicated by red cylinder (α-helix) and blue arrow (β-strand) above the amino acid sequence. In the amino sequence, residues forming α-helix and β-strand of Pba4, PAC3, and Pba3 are indicated as red and blue letters, respectively. Residues boxed in red and black are involved in the α4 and α5 interactions, respectively, with the Pba3–Pba4 heterodimer, as shown by the crystallographic and mutagenesis analyses.[17,18]

model, Pba4, but not Pba3, was involved in interaction with α4, which was mediated through electrostatic interactions involving the residues Lys89, Asp91, and His99 of Pba4. The structural architecture and the charge distribution of these proteasomal subunits are almost identical between human and yeast counterparts (Fig. 2). Although the residues that are involved in α4 interactions in Pba4 are not well conserved in human PAC4 [Fig. 1(C)], surface-charge complementarity is found between PAC4 and α4 from a 3D-structural viewpoint (Fig. 2), suggesting that their interaction mode is evolutionally conserved despite the amino acid substitutions.

To summarize, we report a 1.90-Å resolution crystal structure of the human proteasome-assembling chaperone PAC4. The crystal structure displays complementary surfaces with its binding partner PAC3 and with the cognate proteasomal α4 and α5 subunits, which provides insights into the functional mechanisms of PAC4 in mammalian proteasome assembly. Our current high-resolution structural data offer new clues for designing and developing inhibitors against proteasome biogenesis.

Materials and Methods

Crystallization, X-ray data collection, and structure determination

Recombinant PAC4 was expressed in *E. coli* and purified using immobilized metal affinity and size-

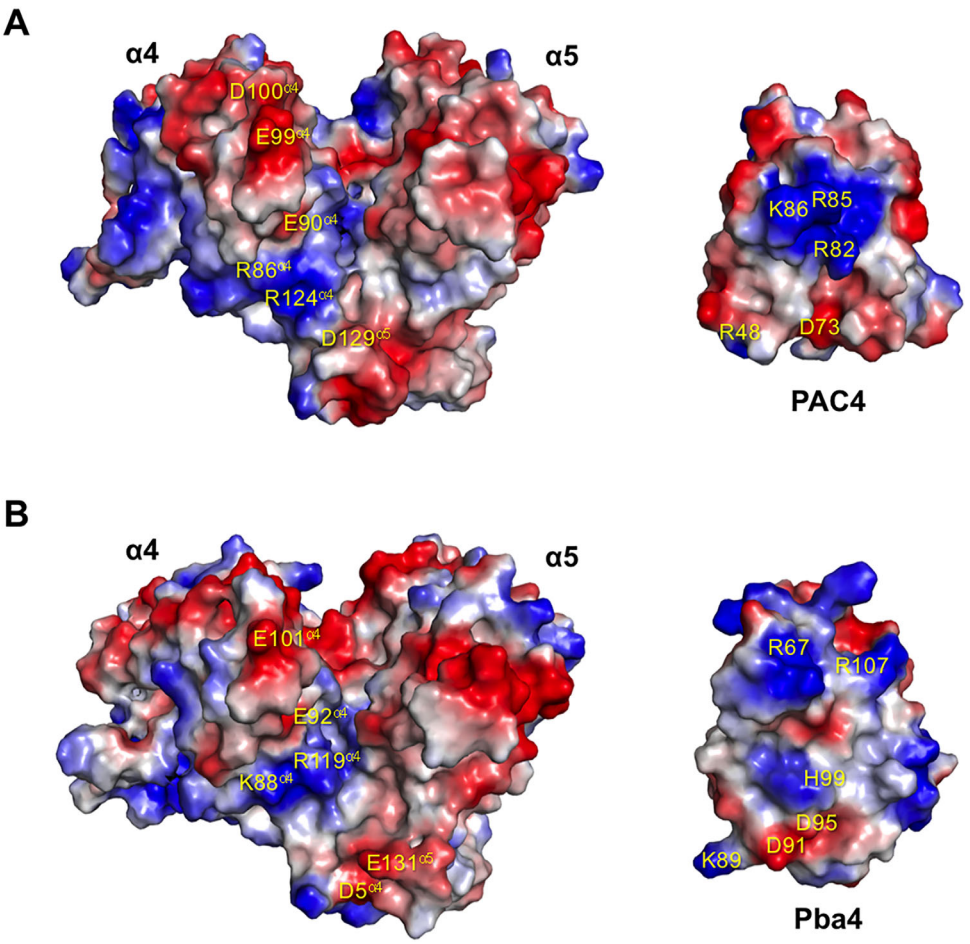

Figure 2. Surface potential representation of (A) human and (B) yeast proteasomal α4 and α5 subunits and the assembly chaperones PAC4/Pba4. The surface models of human (5LE5) and yeast (1RYP) proteasomal α4/α5 complexes (left) and PAC4 orthologs (right) are colored according to the electrostatic surface potential (blue, positive; red, negative). The human α4/α5–PAC4 and yeast α4/α5–Pba4 are shown in an open-book representation.

exclusion chromatography. Further details are provided in the Supporting Information. The non-labeled and SeMet-labeled C55S-PAC4 protein was concentrated to 7 mg/mL in 5 mM Tris-HCl buffer (pH 8.0) and used for crystallization screening. Crystallization screening was performed by the hanging-drop vapor diffusion method using equal volumes of protein and precipitant solutions. After optimization, orthorhombic crystals were obtained by the hanging-drop vapor diffusion method with incubation in a buffer containing 1.0 M lithium sulfate, 0.1 M Tris-HCl (pH 8.5), and 10 mM nickel chloride at 20°C for 3–4 days.

For data collection, the crystals were cryoprotected with the precipitant solution supplemented with 15% glycerol. Diffraction data were collected using synchrotron radiation (0.90000 Å and 0.97932 Å for non-labeled and SeMet-labeled crystals, respectively) at the Osaka University using BL44XU beamline at SPring-8 equipped with MX-300HE (Rayonix). Diffraction data were integrated and scaled using HKL2000.[24] The non-labeled and SeMet-labeled crystals diffracted up to the resolutions of 1.90 Å and 2.60 Å, respectively. The crystallographic parameters are summarized in Table I.

Using the tetragonal 2.60-Å resolution of the SeMet data, the initial coordinates of the PAC4 dimer with the $P4_32_12$ space group were determined using the SAD method with the Phenix AutoSol program.[25] For further model building, molecular replacement was performed against the $F222$ orthorhombic higher resolution native data using MOLREP,[26] in which the tetragonal PAC4 initial model was used as a search model. The high-resolution structures were then built automatically using ARP/wARP,[27] and further model fitting to the electron density maps was performed manually using COOT.[28] The stereochemical quality of the final model was validated using PROCHECK.[29] Refinement statistics are summarized in Table I. The molecular graphics were prepared using PyMOL (http://www.pymol.org/).

Accession Number

The coordinates and structural factor of the crystal structure of PAC4 have been deposited in the PDB under accession number 5WTQ.

Acknowledgments

Diffraction data set was collected at Osaka University using BL44XU beamline at SPring-8. We thank the beamline staff for providing data collection facilities and support.

Conflict of Interest

The authors declare that they have no competing financial interests.

References

1. Tanaka K (2009) The proteasome: overview of structure and functions. Proc Jpn Acad Ser B Phys Biol Sci 85: 12–36.
2. Baumeister W, Walz J, Zühl F, Seemüller E (1998) The proteasome: paradigm of a self-compartmentalizing protease. Cell 92:367–380.
3. Coux O, Tanaka K, Goldberg AL (1996) Structure and functions of the 20S and 26S proteasomes. Annu Rev Biochem 65:801–847.
4. Heinemeyer W, Fischer M, Krimmer T, Stachon U, Wolf DH (1997) The active sites of the eukaryotic 20 S proteasome and their involvement in subunit precursor processing. J Biol Chem 272:25200–25209.
5. Unno M, Mizushima T, Morimoto Y, Tomisugi Y, Tanaka K, Yasuoka N, Tsukihara T (2002) The structure of the mammalian 20S proteasome at 2.75 A resolution. Structure 10:609–618.
6. Lander GC, Estrin E, Matyskiela ME, Bashore C, Nogales E, Martin A (2012) Complete subunit architecture of the proteasome regulatory particle. Nature 482: 186–191.
7. Huang X, Luan B, Wu J, Shi Y (2016) An atomic structure of the human 26S proteasome. Nature Struct Mol Biol 23:778–785.
8. Kish-Trier E, Hill CP (2013) Structural biology of the proteasome. Annu Rev Biophys 42:29–49.
9. Tomko RJ, Jr, Hochstrasser M (2013) Molecular architecture and assembly of the eukaryotic proteasome. Annu Rev Biochem 82:415–445.
10. Murata S, Yashiroda H, Tanaka K (2009) Molecular mechanisms of proteasome assembly. Nature Rev Mol Cell Biol 10:104–115.
11. Nakamura Y, Nakano K, Umehara T, Kimura M, Hayashizaki Y, Tanaka A, Horikoshi M, Padmanabhan B, Yokoyama S (2007) Structure of the oncoprotein gankyrin in complex with S6 ATPase of the 26S proteasome. Structure 15:179–189.
12. Kim S, Saeki Y, Fukunaga K, Suzuki A, Takagi K, Yamane T, Tanaka K, Mizushima T, Kato K (2010) Crystal structure of yeast rpn14, a chaperone of the 19 S regulatory particle of the proteasome. J Biol Chem 285:15159–15166.
13. Takagi K, Kim S, Yukii H, Ueno M, Morishita R, Endo Y, Kato K, Tanaka K, Saeki Y, Mizushima T (2012) Structural basis for specific recognition of Rpt1p, an ATPase subunit of 26 S proteasome, by proteasome-dedicated chaperone Hsm3p. J Biol Chem 287:12172–12182.
14. Barrault MB, Richet N, Godard C, Murciano B, Le Tallec B, Rousseau E, Legrand P, Charbonnier JB, Le Du MH, Guerois R, Ochsenbein F, Peyroche A (2012) Dual functions of the Hsm3 protein in chaperoning and scaffolding regulatory particle subunits during the proteasome assembly. Proc Natl Acad Sci USA 109:E1001–E1010.
15. Ehlinger A, Park S, Fahmy A, Lary JW, Cole JL, Finley D, Walters KJ (2013) Conformational dynamics of the Rpt6 ATPase in proteasome assembly and Rpn14 binding. Structure 21:753–765.
16. Satoh T, Saeki Y, Hiromoto T, Wang YH, Uekusa Y, Yagi H, Yoshihara H, Yagi-Utsumi M, Mizushima T, Tanaka K, Kato K (2014) Structural basis for proteasome formation controlled by an assembly chaperone nas2. Structure 22:731–743.
17. Yashiroda H, Mizushima T, Okamoto K, Kameyama T, Hayashi H, Kishimoto T, Niwa S, Kasahara M, Kurimoto E, Sakata E, Takagi K, Suzuki A, Hirano Y, Murata S, Kato K, Yamane T, Tanaka K (2008) Crystal structure of a chaperone complex that contributes to the assembly of yeast 20S proteasomes. Nature Struct Mol Biol 15:228–236.
18. Takagi K, Saeki Y, Yashiroda H, Yagi H, Kaiho A, Murata S, Yamane T, Tanaka K, Mizushima T, Kato K (2014) Pba3-Pba4 heterodimer acts as a molecular matchmaker in proteasome α-ring formation. Biochem Biophys Res Commun 450:1110–1114.
19. Kusmierczyk AR, Kunjappu MJ, Funakoshi M, Hochstrasser M (2008) A multimeric assembly factor controls the formation of alternative 20S proteasomes. Nature Struct Mol Biol 15:237–244.
20. Almond JB, Cohen GM (2002) The proteasome: a novel target for cancer chemotherapy. Leukemia 16:433–443.
21. Doi T, Yoshida M, Ohsawa K, Shin-ya K, Takagi M, Uekusa Y, Yamaguchi T, Kato K, Hirokawa T, Natsume T (2014) Total synthesis and characterization of thielocin B1 as a protein–protein interaction inhibitor of PAC3 homodimer. Chem Sci 5:1860. 1868.
22. Zhang X, Schulz R, Edmunds S, Kruger E, Markert E, Gaedcke J, Cormet-Boyaka E, Ghadimi M, Beissbarth T, Levine AJ, Moll UM, Dobbelstein M (2015) MicroRNA-101 suppresses tumor cell proliferation by acting as an endogenous proteasome inhibitor via targeting the proteasome assembly factor POMP. Mol Cell 59: 243–257.
23. Le Tallec B, Barrault MB, Courbeyrette R, Guérois R, Marsolier-Kergoat MC, Peyroche A (2007) 20S proteasome assembly is orchestrated by two distinct pairs of chaperones in yeast and in mammals. Mol Cell 27:660–674.
24. Otwinowski Z, Minor W (1997) Processing of X-ray diffraction data collected in oscillation mode. Methods Enzymol 276:307–326.
25. Adams PD, Afonine PV, Bunkoczi G, Chen VB, Davis IW, Echols N, Headd JJ, Hung LW, Kapral GJ, Grosse-Kunstleve RW, McCoy AJ, Moriarty NW, Oeffner R, Read RJ, Richardson DC, Richardson JS, Terwilliger TC, Zwart PH (2010) PHENIX: a comprehensive Python-based system for macromolecular structure solution. Acta Cryst D66:213–221.
26. Vagin A, Teplyakov A (1997) MOLREP: An automated program for molecular replacement. J Appl Cryst 30: 1022–1025.
27. Langer G, Cohen SX, Lamzin VS, Perrakis A (2008) Automated macromolecular model building for X-ray crystallography using ARP/wARP version 7. Nat Protoc 3:1171–1179.
28. Emsley P, Lohkamp B, Scott WG, Cowtan K (2010) Features and development of Coot. Acta Cryst D66: 486–501.
29. Laskowski RA, MacArthur MW, Moss DS, Thornton JM (1993) PROCHECK: a program to check the stereochemical quality of protein structures. J Appl Cryst 26: 283–291.